

Original Research

EIF2Ss, a Novel c-Myc-Correlated Gene Family, is Associated with Poor Prognosis and Immune Infiltration in Pancreatic Adenocarcinoma

Zhangqi Cao^{1,2,†}, Yanhua Jing^{1,2,†}, Chien Shan Cheng^{1,2}, Fengjiao Wang^{1,2}, Mingwei Guan^{1,2},
Ke Zhang^{1,2}, Juying Jiao^{1,2}, Linjie Ruan^{1,2}, Zhen Chen^{1,2,*}¹Department of Integrative Oncology, Fudan University Shanghai Cancer Center, 200032 Shanghai, China²Department of Oncology, Shanghai Medical College, Fudan University, 200032 Shanghai, China*Correspondence: zchenzl@fudan.edu.cn (Zhen Chen)

†These authors contributed equally.

Academic Editor: Elisa Belluzzi

Submitted: 10 March 2023 Revised: 14 October 2023 Accepted: 20 October 2023 Published: 21 March 2024

Abstract

Background: Pancreatic adenocarcinoma (PAAD) is a highly malignant tumor in urgent need of novel diagnostics, prognostic markers, and treatments. Eukaryotic translation initiation factor 2 subunits (EIF2Ss), comprising Eukaryotic translation initiation factor 2 subunit alpha (EIF2S1), Eukaryotic translation initiation factor 2 subunit beta (EIF2S2), and Eukaryotic translation initiation factor 2 subunit gamma (EIF2S3), is a family of eukaryotic initiation factors that participate in early protein synthesis and are crucial for tumor initiation and progression. However, the role of EIF2Ss in PAAD has yet to be reported. The aim of this study was therefore to analyze EIF2Ss in relation to the diagnosis, prognosis, and treatment of PAAD. **Methods:** The cancer genome atlas (TCGA) database was used to investigate gene expression and patient survival. Gene alterations, immune cell infiltration, and immune checkpoints in PAAD were also evaluated. Univariate and multivariate analysis, nomograms, calibration curves, and Decision Curve Analysis (DCA) diagrams were used to develop and evaluate a prediction model for patient outcome. Single-cell RNA-seq (scRNA) analysis, functional enrichment, co-IP assay, mass spectrometry, and western blot were used to study the relationship between EIF2Ss and c-myc in PAAD. **Results:** EIF2Ss are over-expressed in PAAD tissue and are associated with poor prognosis. The frequency of *EIF2S1*, *EIF2S2*, and *EIF2S3* gene alteration in PAAD was 0.2%, 0.4%, and 0.2%, respectively. High EIF2Ss expression was associated with Th2 cell infiltration, whereas low expression was associated with pDC infiltration. Moreover, EIF2Ss expression was positively correlated with the expression of the *NTSE*, *ULBP1*, *PVR*, *CD44*, *IL10RB*, and *CD276* checkpoints. A prediction model developed using EIF2Ss and important clinicopathologic features showed good predictive value for the overall survival of PAAD patients. ScRNA-Seq data showed that EIF2Ss was associated with enrichment for endothelial cells, fibroblasts, malignant cells, and ductal cells. EIF2Ss expression was also correlated with adipogenesis, interferon-alpha response, epithelial-mesenchymal transition, myc targets, G2M checkpoint, oxidative phosphorylation, and hypoxia. Functional enrichment analysis of EIF2Ss showed a close correlation with the myc pathway, and interactions between EIF2Ss and c-myc were confirmed by co-IP assay and mass spectrometry. Importantly, knockdown of c-myc decreased the expression of EIF2S1, EIF2S2, and EIF2S3 in PAAD cells. **Conclusions:** EIF2Ss were found to have significant clinical implications for the prognosis and treatment of PAAD. Inhibition of c-myc caused the downregulation of EIF2S1, EIF2S2, and EIF2S3 expression.

Keywords: EIF2Ss; pancreatic adenocarcinoma; prognosis; immune infiltration; c-myc

1. Introduction

Pancreatic adenocarcinoma (PAAD) is a highly malignant tumor with poor prognosis [1,2]. Despite extensive research efforts to identify novel diagnostic and prognostic biomarkers, most patients with PAAD are diagnosed at an advanced stage [3–5]. Furthermore, there are no effective therapeutic approaches for PAAD other than surgical resection, and hence the overall survival (OS) and progression free survival (PFS) of patients with this cancer type remains extremely poor [6,7]. Hence, there is an urgent need to find new diagnostic markers and therapeutic targets for PAAD that will allow early diagnosis and target-specific treatment.

Eukaryotic translation initiation factor 2 is composed of three subunits, namely eukaryotic translation initiation factor 2 subunit alpha (EIF2S1), beta (EIF2S2), and gamma

(EIF2S3) [8,9]. These subunits are heavily involved in the early stages of protein synthesis, and are also thought to belong to a family of oncogenes [10,11]. Overexpression of EIF2S1 was reported to promote tumorigenesis of human lymphoma and neuroblastoma, and to be closely associated with the OS of these patients [12,13]. EIF2S2 is crucial for the formation of pre-synthesis protein initiation complexes, thereby supporting the high protein demand that occurs during organelle synthesis in cancer cells [14]. EIF2S2 was also identified as a novel prognosis marker and as part of strategy for combination therapy [15,16]. EIF2S3 is the largest subunit of EIF2S and plays a decisive role in controlling the protein translation rate [17–19]. Overexpression of EIF2S3 was found in both the peripheral blood and tumor tissues of PAAD patients [20], making it a non-invasive



marker for diagnosis and prognosis. However, possible role for EIF2Ss in the diagnosis, treatment, and prognosis of PAAD have yet to be not been comprehensively investigated.

In the present study, we therefore evaluated the expression of EIF2Ss in PAAD, as well as their diagnostic and prognostic significance. We also built a prognostic model based on EIF2Ss that showed good prediction of survival for PAAD patients. Importantly, knockdown of c-myc expression was observed to downregulate the expression of EIF2S1, EIF2S2, and EIF2S3 in PAAD cells. Overall, these research findings on EIF2Ss overexpression suggest new options for improving the diagnosis, prediction of outcome, and treatment of PAAD patients.

2. Materials and Methods

2.1 Data Collection and Processing

RNA-seq data (TPM) for 730 para-cancerous tissue samples and 10,363 pan-cancer samples were obtained from the Cancer Genome Atlas (TCGA) database (<http://portal.gdc.cancer.gov/repository>). For PAAD, 4 para-cancerous tissue samples and 179 cancer samples were downloaded from the TCGA Knowledge Base. Furthermore, 167 normal samples were retrieved from University of California Santa Cruz Xena (UCSC Xena, <http://xena.ucsc.edu/>) take into account sample heterogeneity.

2.2 Gene Alterations

Gene alteration data including alteration frequency, possible mutation sites, and alteration type were obtained from the cBioPortal database (<https://www.cbioportal.org/>). Details of the gene alteration types, such as amplification, missense mutation, and deep deletion of the genes were also examined.

2.3 Analysis of Immune Cell Infiltration

Immune cell infiltration and target gene expressions in PAAD was assessed using R (v 3.6.3, The R Foundation for Statistical Computing, Vienna, Austria). The Tumor Immune Estimation Resource (TIMER) database (<https://cistrome.shinyapps.io/timer/>) was used to examine correlations between immune cell infiltration and gene copy number variations, and also between immune cell infiltration and gene expression levels. The Tumor-Immune System Interactions Database (TISIDB) (<http://cis.hku.hk/TISIDB/>) was used to analyze gene expression in different immune cell subtypes, as well as correlations with lymphocytes and immunostimulators. The correlation between 70 common checkpoints and target genes was analyzed with R software (v 3.6.3).

2.4 Nomogram Construction

Univariate and multivariate Cox regression analyses were used to identify appropriate genes for constructing a nomogram. The parameters included T stage, N stage,

pathological stage, radiation therapy, residual tumor, histological grade, anatomic neoplasm subdivision, and the expression of *EIF2S1*, *EIF2S2*, and *EIF2S3*. Receiver Operating Characteristic (ROC) curves, Kaplan-Meier survival curves, calibration curves, and Decision Curve Analysis (DCA) diagrams were used to evaluate the predictive ability of the prognostic model for patient survival.

2.5 scRNA Analysis

A scRNA-seq data source, tumor immune single-cell hub (TISCH) (<http://tisch.comp-genomics.org/home/>), focuses on the tumor microenvironment (TME) and provides cell-type specific annotations at the single-cell level, thereby enabling research on TME in various types of malignancies. The TISCH was used to analyze PAAD scRNA data obtained from the CRA001160 and GSE111672 databases. EIF2Ss expression in various cell types were shown in T-SNE projection. The enrichment of cells in various pathways was also shown in TISCH.

2.6 Correlation of Related Genes and Enrichment Analysis

Gene Set Enrichment Analysis (GSEA) is a previously established gene collection that shows statistically significant and continuous changes between two biological states using a computerized method (<https://www.gsea-msigdb.org/gsea/index.jsp>). This was used to find all genes that have been linked to *EIF2Ss* gene expression in previous research and to investigate for possible survival differences between high and low expression groups. Gene set permutation was conducted 1000 times for each analysis. Highly correlated genes were illustrated by heatmap using the R package (version 3.3.3, ggplot2). The genes and correlated genes were enriched using GSEA.

2.7 Cell Culture and Quantitative Real Time Polymerase Chain Reaction (qRT-PCR)

The human pancreatic cancer cell lines SW1990 and Capan1 were purchased from the American Type Culture Collection (Manassas, VA, USA). Short Tandem Repeat (STR) profiling was used to authenticate the cell lines, and all cells tested free of mycoplasma. Both cell lines were cultured in an incubator at 37 °C with 5% CO₂ incubator and grown in Dulbecco's Modified Eagle Medium (DMEM) (Sigma-Aldrich, St. Louis, MO, USA) containing 1% penicillin (Sigma-Aldrich), 1% streptomycin (Sigma-Aldrich), and 10% fetal bovine serum (Hyclone; Cytiva, Logan, UT, USA). The total RNA of pancreatic cancer cells was extracted by TRIzol Reagent (Invitrogen, Carlsbad, CA, USA). The reverse transcription of total RNA to DNA was completed by the TaKaRa PrimeScript RT Reagent Kit (TaKaRa, Kusatsu, Japan). SYBR Green Real-Time PCR Master Mixes (Yeasen Biotechnology, Shanghai, China) was used to detect the expression of *EIF2S1*, *EIF2S2*, and *EIF2S3*. The GAPDH served as an internal reference control.

2.8 Co Immunoprecipitation (Co-IP) and Western Blot

SW1990 and Capan1 pancreatic cancer cells were washed twice with PBS, then cell lysis buffer (Beyotime, Shanghai, China) supplemented with protease and phosphatase inhibitors (Beyotime, Shanghai, China) was added, and the dish was placed on ice for 30 minutes. Cells were scraped by a pre-cooled cell scraper and the suspension transferred to a 1.5 mL EP tube and centrifuged at 14,000 g for 15 minutes at 4 °C. The cell lysate supernatant was immediately transferred to a new 1.5 mL EP tube and the relative protein concentration measured with a BCA Protein Assay kit (Beyotime, Shanghai, China). A small amount of cell lysate supernatant was taken as input. The corresponding antibody was then added to the remaining cell lysate supernatant and incubated for 24 hours at 4 °C. Next, 50 µL protein A/G magnetic beads (Beyotime, Shanghai, China) were incubated with the complex overnight at 4 °C and then washed with lysis buffer. Finally, the input, IgG, and IP fractions were subjected to western blot analysis. Following electrophoresis with 10% SDS-PAGE, the proteins were transferred onto polyvinylidene difluoride (PVDF) membranes. The membranes were then treated with the following primary antibodies: c-Myc (1:1000, Proteintech, Chicago, IL, USA), EIF2S1 (1:1000, Proteintech), EIF2S2 (1:1000, Proteintech), EIF2S3 (1:1000, Proteintech), and glyceraldehyde-3-phosphate dehydrogenase (GAPDH) (1:1000, Proteintech). These antibodies were treated with the PVDF membrane overnight, washed, and then incubated with a Horseradish Peroxidase (HRP)-labeled secondary antibody solution for 1 hour. Finally, enhanced chemiluminescence (ECL) luminescent solution was added to the surface of the PVDF membranes, to visualize the immunoblot bands in a pre-cooled LAS4000 luminescent imager (GE, Boston, MA, USA).

2.9 LC-MS/MS Quantification

Pancreatic cancer cells were harvested, lysed with cell lysis buffer, and then quantified and labeled as the input sample. The IP sample was separated by SDS-PAGE, and LC-MS/MS analysis was then performed (Shanghai Genechem Co., Ltd.). Briefly, the bands from SDS-PAGE were divided into 1 mm³ for each gel slice. The proteins were then dissolved, and the peptide samples were desalted and resuspended. Easy nLC chromatography was subsequently performed, with 0.1% formic acid aqueous solution used as buffer A and 0.1% formic acid acetonitrile aqueous solution used as buffer B. A nanoliter flow rate Easy nLC system was used to separate the experimental samples, which were then subjected to mass spectrometry analysis using a Q Active Plus mass spectrometer (Thermo Fisher Scientific, MA, USA). Finally, the original graph file obtained from Q Active Plus was converted, processed, and analyzed.

2.10 Statistical Analysis

Data were analyzed using R software version 3.6.3 (The R Foundation for Statistical Computing, Vienna, Austria), SPSS 20.0 (IBM Corp. Released 2011. IBM SPSS Statistics for Windows, Version 20.0. IBM Corp., Armonk, NY, USA), and GraphPad Prism 8.0.0 (GraphPad Prism version 8.0.0 for Windows, GraphPad Software, Boston, MA, USA, <https://www.graphpad.com/>). Student's *t*-test or one-way ANOVA were used to compare groups, and a *p*-value < 0.05 was deemed statistically significant.

3. Results

3.1 Expression of EIF2Ss in PAAD and Their Diagnostic and Prognostic Value

The expression of EIF2Ss and their prognostic value in many different cancer types were examined using TCGA data. The expression of EIF2S1, EIF2S2, and EIF2S3 were elevated in tumor tissue compared to the corresponding normal tissue (**Supplementary Fig. 1A–C**). These genes were also consistently overexpressed in PAAD (Fig. 1A–C). Kaplan-Meier analysis revealed that high expression of EIF2S1, EIF2S2 and EIF2S3 in PAAD patients was associated with poor OS (Fig. 1D–F), disease-specific survival (DSS) (**Supplementary Fig. 1D**), and progress-free interval (PFI) (**Supplementary Fig. 1E**). The area under the curve (AUC) for ROC analysis of EIF2S1, EIF2S2 and EIF2S3 expression were 0.926, 0.971, and 0.881, respectively (Fig. 1G–I). Moreover, time-dependent ROC curves for EIF2Ss showed AUCs of 0.614, 0.646, and 0.754 for EIF2S1 (**Supplementary Fig. 1F**), 0.674, 0.629, and 0.620 for EIF2S2 (**Supplementary Fig. 1F**), and 0.586, 0.655, and 0.760 for EIF2S3 (**Supplementary Fig. 1F**).

We next examined the clinicopathological characteristics of PAAD groups with differentially expressed EIF2Ss. Patients with high expression of EIF2S1 presented with T3/T4 stage, stage II/III/IV, PD, and G2/G3/G4 grades (**Supplementary Fig. 2A–D**). Patients with high EIF2S2 expression presented with PD and G2/G3/G4 grades (**Supplementary Fig. 2E,F**). Patients with high expression of EIF2S3 presented with T3/ T4 stage, female gender, residual tumor R1 and R2, and G2/G3/G4 grade (**Supplementary Fig. 2G–J**). Possible associations between OS with clinical characteristics and EIF2Ss were also investigated. High expression of EIF2S1 in patients with T1/T2, N0, no radiotherapy, male, residual tumor R0, G1/G2 grade, diabetes history and no family history of cancer was associated with poor OS (**Supplementary Fig. 3A**). Low EIF2S2 expression in PAAD patients with T1/T2, M0, P0, no radiation, PD, male, white, R1/R2 residual tumor, G1/G2 grade, pancreatic cancer head, no alcohol history, and no cancer family history of cancer was associated with good OS (**Supplementary Fig. 3B**). Furthermore, poor OS was observed with high expression of EIF2S3 in pancreatic cancer patients with N0 stage, no radiation ther-

apy, less than or equal to 65 years old, residual tumor of R1/R2, G1/G2 grade, no smoker, and history of diabetes (**Supplementary Fig. 3C**).

3.2 *EIF2Ss Gene Alterations in PAAD*

Data on EIF2Ss gene alterations were obtained from the cBioPortal database. The distribution of alteration types is shown in Fig. 2A–C. EIF2S1 and EIF2S2 showed amplification and deep deletions (Fig. 2D,E), whereas EIF2S3 showed missense mutations and deep deletions (Fig. 2F).

3.3 *EIF2Ss and Immune Infiltration in PAAD*

PAADs with high levels of EIF2Ss expression were infiltrated with Th2 cells (Fig. 3A–C). In contrast, PAADs with a low level of EIF2Ss expression were infiltrated with pDC (Fig. 3A–C). High levels of EIF2S1 and EIF2S3 expression were associated with infiltration by T helper cells and Th2 cells (Fig. 3A,C). Low EIF2S2 expression was associated with infiltration by CD8+ T cells, cytotoxic cells, iDC, mast cells, NK cells, pDC, T cells, TFH, Th17 cells, and Th2 cells (Fig. 3B). The relationship between immune cell infiltration and EIF2Ss expression was also investigated using the TIMER database. EIF2S1, EIF2S2, and EIF2S3 expression were all positively associated with CD8+ T cells (Fig. 3D–F). In addition, EIF2S1 expression was positively associated with B cells, macrophages, neutrophils, and DCs (Fig. 3D). EIF2S3 expression was positively associated with B cells, neutrophils, and DCs (Fig. 3F).

3.4 *EIF2Ss Correlations with Immune Checkpoints, Subtypes, Lymphocytes, and Immunostimulators*

Correlations between the expression levels of EIF2S1, EIF2S2, and EIF2S3 with the expression of 70 common immune checkpoints in PAAD are presented in Fig. 4A. The expression of EIF2S1 was positively associated with CD44, NT5E, CD274, IL2RA, NRP1, ENTPD1, CD86, PDCD1LG2, PVR, TGFBR1, TNFSF4, TNFSF13B, CD80, ULBP1, CD276, HAVCR2, MICB, CSF1R, CD28, RAET1E, ICOS, TIGIT, TNFRSF9, LAIR1, CD96, IL10, CD200R1, CXCR4, TNFSF18, IL10RB, IL6, TNFSF15, IDO1, CD70 and CD244 (**Supplementary Fig. 4A**). The expression of EIF2S2 was positively associated with NT5E, ULBP1, PVR, CD44, IL10RB and CD276 (**Supplementary Fig. 4B**). Finally, the expression of EIF2S3 was positively correlated with that of CD44, NT5E, MICB, IL2RA, TNFSF4, CD274, NRP1, PDCD1LG2, TNFSF13, ENTPD1, TNFSF13B, RAET1E, TNFRSF9, TNFRSF15, CD86, TGFBR1, ICOS, TIGIT, CD40, CD96, CD80, CD28, CD276, HAVCR2, CD200R1 and IDO1 (**Supplementary Fig. 4C**). The expression levels of EIF2S1, EIF2S2, and EIF2S3 in PAAD also correlated with the immune subtypes C1 (wound healing), C2 (IFN-gamma dominant), C3 (Inflammatory), and C6 (TGF- β dominant) (Fig. 4B–D).

A heatmap generated with the TISIDB database showed the correlations between EIF2Ss, lymphocytes and immunostimulators in 30 cancer types (**Supplementary Fig. 5A–F**). In PAAD, most lymphocytes and immunostimulators were positively correlated with the expression of EIF2S1, EIF2S2, and EIF2S3. The expression of EIF2S1 was also positively correlated with an abundance of Act—CD4 cells, Tcm—CD4 cells, Tcm—CD8 cells, and Th2 cells (**Supplementary Fig. 5G–J**). EIF2S2 and EIF2S3 expression were positively associated with an abundance of CD56dim cells and Act CD4 cells, respectively (**Supplementary Fig. 5M,O**). EIF2S1 expression was also positively correlated with expression of the IL2RA and NT5E immunostimulators (**Supplementary Fig. 5K,L**). Finally, the expression of EIF2S2 was positively associated with NT5E (**Supplementary Fig. 5N**).

3.5 *Construction of a Nomogram for PAAD*

Optimization of a prognostic model for patient outcome could improve its accuracy and therefore its clinical value, especially in PAADs with high expression of EIF2Ss. We therefore built a model using univariate and multivariate Cox regression analysis, and incorporated important clinicopathologic features (T stage, N stage, pathological stage, radiation therapy, residual tumor, histologic grade, anatomic neoplasm subdivisions), as well as EIF2Ss (**Supplementary Fig. 6A,B**). This nomogram was predictive of 1-year, 2-year, and 3-year OS probability (Fig. 5A). Subsequently, the predictive efficacy and value of the nomogram were verified by ROC curves, calibration curves, and DCA diagrams. The AUC of ROC curves for 1-year, 2-year, and 3-year OS were 0.749, 0.824, and 0.807, respectively (Fig. 5B). Furthermore, the calibration curves (Fig. 5C–E) and DCA diagram (Fig. 5F–H) showed good consistency between the prediction and the actual state.

3.6 *scRNA-Seq Analysis of EIF2S1, EIF2S2, and EIF2S3 in PAAD*

Correlations between immune cell infiltration and EIF2Ss expression were further verified by scRNA-Seq data obtained from PAAD_CRA001160 and PAAD_GSE111672 (Fig. 6A,E). The results showed that EIF2S1, EIF2S2, and EIF2S3 were highly expressed in endothelial cells, fibroblasts, malignant cells, and ductal cells (Fig. 6B–D,F–K). Enrichment analysis of EIF2Ss in PAAD_CRA001160 and PAAD_GSE11167 indicated that adipogenesis and interferon-alpha response were mainly associated in endothelial cells; the epithelial-mesenchymal transition was mainly associated in fibroblasts; myc targets, G2M checkpoint, and interferon-alpha response were mainly enriched in malignant cells; oxidative phosphorylation, interferon-alpha response, and hypoxia were mainly enriched in ductal cells (**Supplementary Figs. 7,8**).

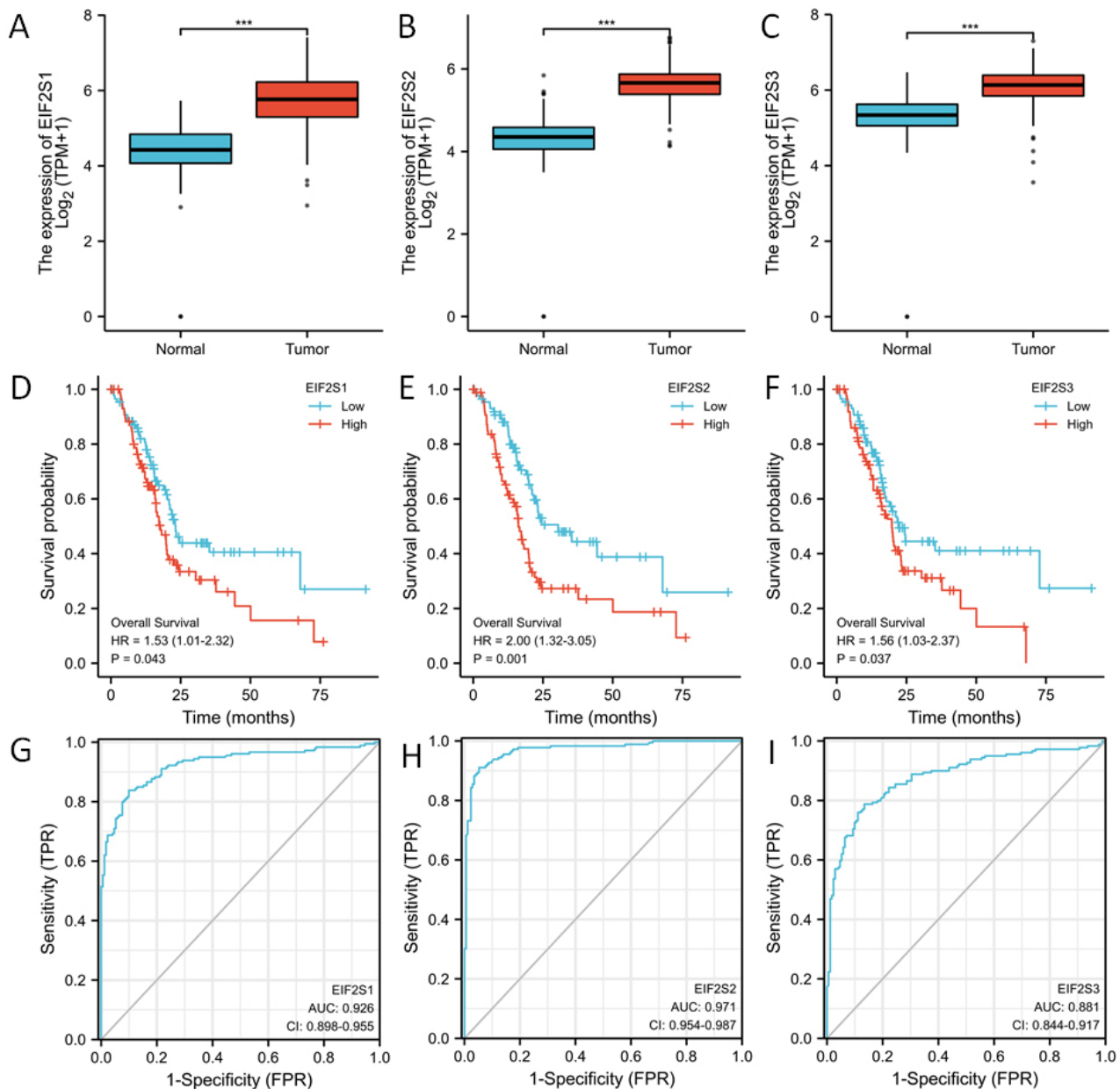


Fig. 1. Expression of EIF2Ss in Pancreatic adenocarcinoma (PAAD) and their prognostic and diagnostic value. (A–C) Differential expression of EIF2S1, EIF2S2, and EIF2S3 in PAAD tumor and normal tissue. (D–F) OS curves for PAAD patients with low ($n = 89$) or high ($n = 90$) expression levels of EIF2S1, EIF2S2, and EIF2S3. (G–I) ROC curves indicate the diagnostic value of EIF2S1, EIF2S2, and EIF2S3 expression in PAAD. $***p < 0.001$. PAAD, pancreatic adenocarcinoma; EIF2S1, eukaryotic translation initiation factor 2 subunit alpha; EIF2S2, eukaryotic translation initiation factor 2 subunit beta; EIF2S3, eukaryotic translation initiation factor 2 subunit gamma; OS, overall survival; ROC, receiver operating characteristic; AUC, area under the curve; CI, confidence interval.

3.7 Correlations between EIF2Ss and c-Myc in PAAD

The scRNA-Seq data analysis in PAAD showed that myc targets were enriched in malignant cells with EIF2Ss expression. Hence, interactions between EIF2Ss and c-myc were further investigated. The results of GSEA functional enrichment analysis are shown in Fig. 7A–C. The spearman correlation coefficients for EIF2S1, EIF2S2, and EIF2S3 with c-myc were 0.488, 0.255, and 0.4, re-

spectively (Fig. 7D–F). Myc was upregulated in tumor tissue compared with normal tissue (Fig. 7G). Kaplan-Meier analysis showed that high myc expression was associated with poor OS (Fig. 7H). Mass spectrum analysis confirmed that EIF2S1, EIF2S2, and EIF2S3 proteins were co-immunoprecipitated with myc (Fig. 7I). The mass spectrogram showed the EIF2S1 peptide sequence was GVFNVQMEPK (Fig. 7J), the EIF2S2 peptide sequence was EYVTCHTCR (Fig. 7K), the EIF2S3 pep-

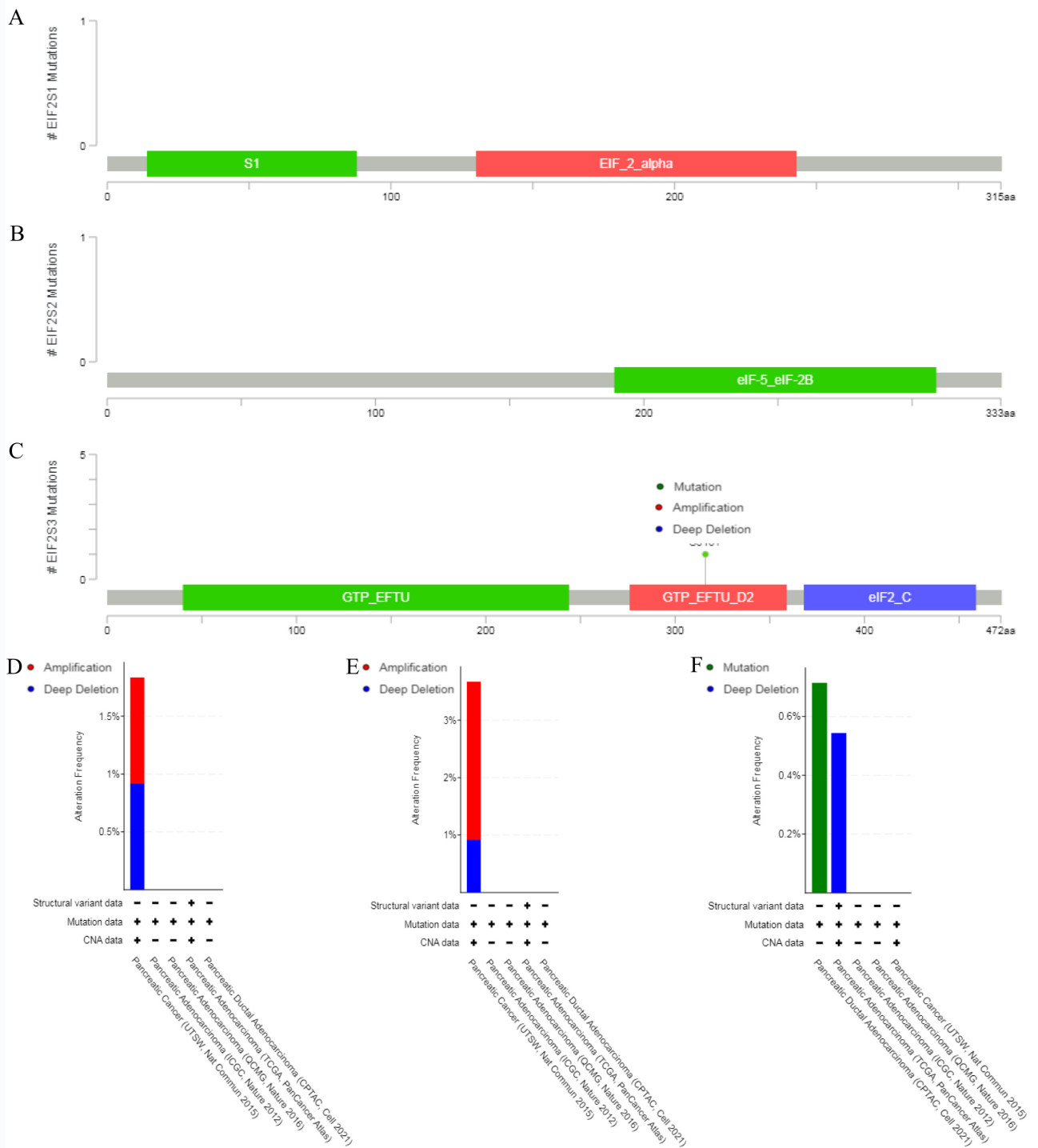


Fig. 2. EIF2Ss gene alterations in PAAD. (A–C) The location of gene alteration types in EIF2S1, EIF2S2 and EIF2S3. (D–F) Gene alteration types and proportions in EIF2S1, EIF2S2, and EIF2S3.

tide sequence was VGQEIEVRPGIVSK (Fig. 7L). Co-immunoprecipitation experiments using SW1990 and Capn1 cell lysis protein were used to further confirm the interaction between c-myc and EIF2Ss, c-myc was again found to co-immunoprecipitate with EIF2S1, EIF2S2, and EIF2S3 (Fig. 7M). Western blot analysis also showed that EIF2S1, EIF2S2, and EIF2S3 co-immunoprecipitated with

c-myc (Fig. 7N). Moreover, knock down of c-myc was observed to downregulate the expression of EIF2S1, EIF2S2, and EIF2S3 (Fig. 7O). Overexpression of c-myc was observed to upregulate the expression of EIF2S1, EIF2S2, and EIF2S3 (Fig. 7P). In the meanwhile, the RT-qPCR results were also verified this point (Fig. 7Q–R).

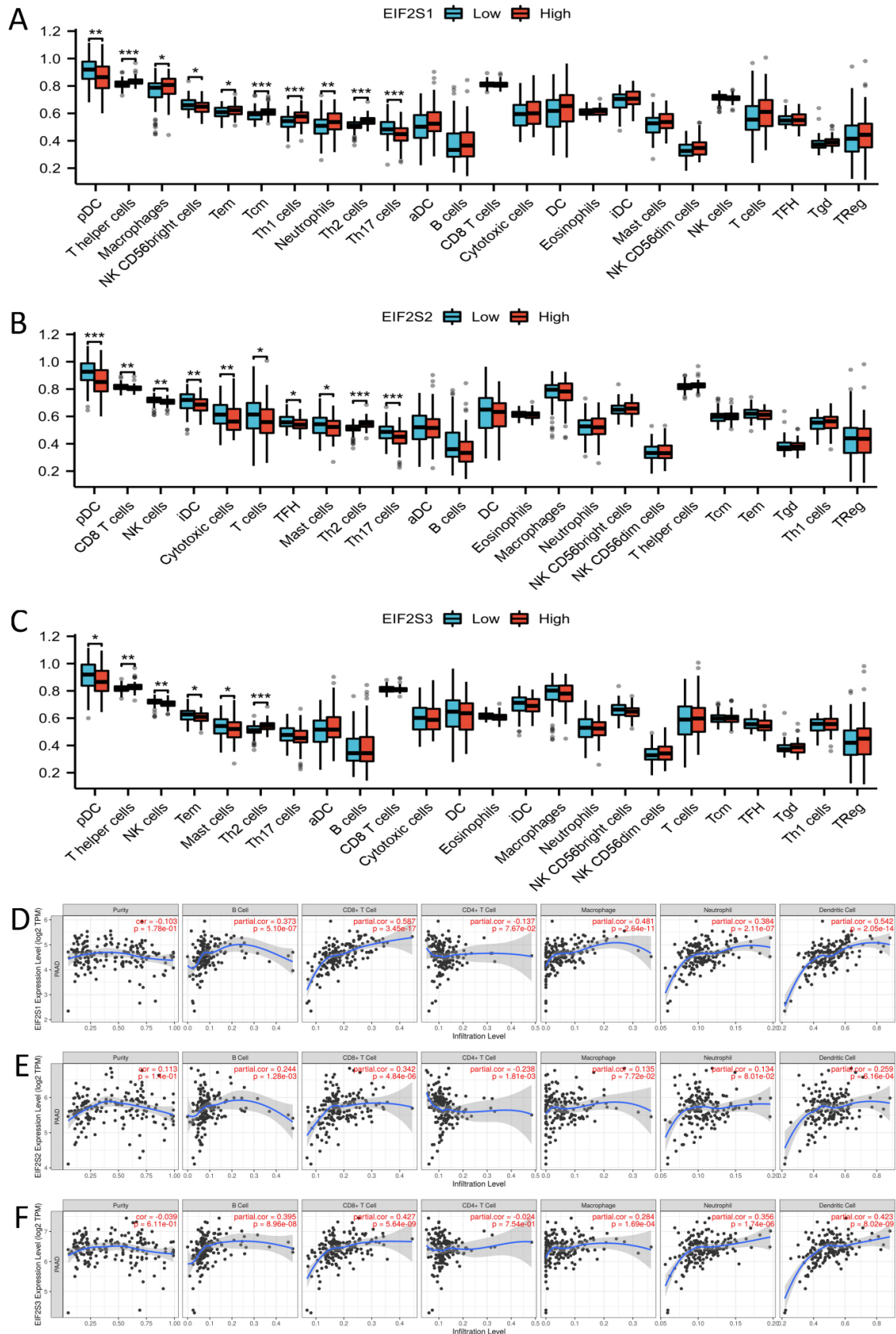


Fig. 3. Immune infiltration and EIF2Ss in PAAD. (A–C) Immune cells enrichment in PAAD with low or high expression of EIF2S1, EIF2S2, and EIF2S3. (D–F) Immune cell enrichment in copy number variations (CNVs) of EIF2S1, EIF2S2, and EIF2S3. * $p < 0.05$, ** $p < 0.01$ and *** $p < 0.001$.

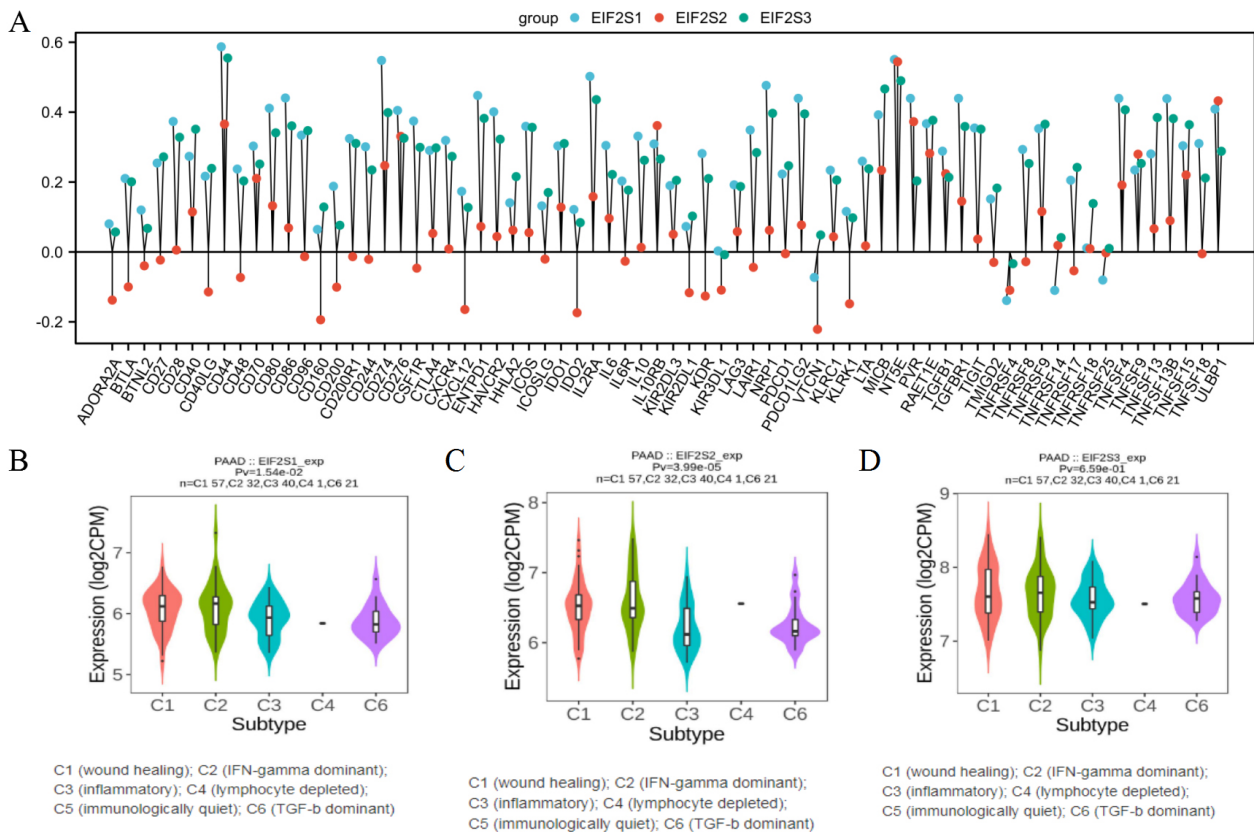


Fig. 4. EIF2Ss correlations with immune checkpoints, subtypes, lymphocytes, and immunostimulators. (A) Correlations between the expression of 70 common immune checkpoints and the expression of EIF2S1, EIF2S2, and EIF2S3 in PAAD. (B–D) Correlations between EIF2S1, EIF2S2, and EIF2S3 expression and immune subtypes.

4. Discussion

Despite advances in surgery, chemotherapy, targeted therapy, and immunotherapy, the outcome for PAAD patients remains poor [21]. The OS of PAAD patients is generally much shorter than that of other tumor types, partly due to the late onset of clinical symptoms and diagnosis [22]. Furthermore, the occult characteristics of PAAD, high tumor heterogeneity, and strong resistance to drug therapy and immunotherapy all contribute to its poor prognosis [23,24].

In the present work, we comprehensively studied the diagnostic, prognostic, and treatment significance of EIF2Ss in PAAD. Our results show that EIF2S1, EIF2S2, and EIF2S3 are highly expressed in the tumor tissue of PAAD compared with corresponding normal tissue, while also being associated with worse prognosis. EIF2Ss are important gene family that combined with GTP and initiator tRNA to form a 40S ribosomal subunit that functions in the early stages of protein synthesis [25–27]. Correlations between members of EIF2Ss and various other tumor types have been reported previously. Both in silico and immunohistochemical studies reported high expression of EIF2S1 and EIF2S2 in intestinal-type adenocarcinoma [28]. EIF2S1 was shown to interact with ERh and to

up-regulate the expression of ATF4 and CHOP mRNA in bladder cancer [29]. EIF2S2 was associated with the clinicopathological characteristics and poor prognosis of HCC [30]. Moreover, the mRNA level of EIF2S2 in colorectal cancer (CRC) was consistent with immunohistochemistry findings and closely correlated with Fluorodeoxyglucose (FDG) uptake [31]. The blood EIF2S3 expression level was proposed as a marker for blood-based detection assays in CRC patients [32]. All of the above studies found that EIF2Ss were upregulated in the tumor tissues or blood samples of patients with various cancer types. However, the expression levels of EIF2S1, EIF2S2, and EIF2S3 in PAAD have not yet been reported. The present research first found that EIF2S1, EIF2S2, and EIF2S3 are highly expressed in PAAD compared with normal tissue, and have significant prognostic value for OS in this cancer type. Moreover, patients with histological grade G2, G3, and G4 tumors showed high expression of EIF2S1, EIF2S2, and EIF2S3. The high expression of EIF2Ss family members has been associated with a higher degree of pathological malignancy, thereby indicating poor prognosis and patient outcome. Patients with T3 or T4 stage tumors in the present study also showed higher expression of EIF2S1 and EIF2S3 than those with T1 or T2 stage tumor, again indicating that elevated

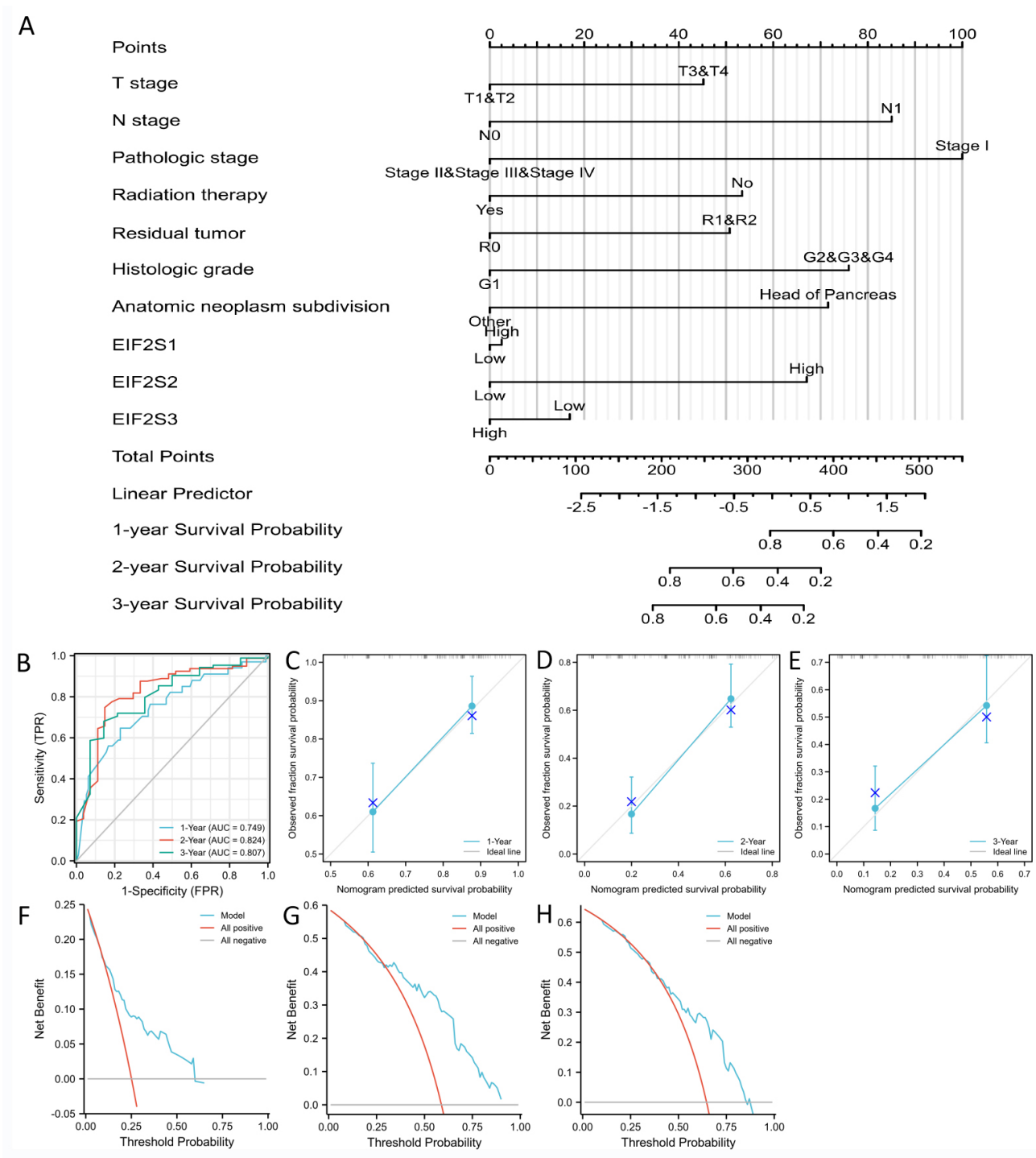


Fig. 5. Construction of a nomogram for PAAD. (A) The nomogram was used to predict the OS of PAAD patients at 1-year, 2-year, and 3-years. (B) ROC curves indicate the diagnostic value of the nomogram. (C–E) Calibration curves for the nomogram predict OS at 1-year, 2-year, and 3-years. (F–H) Decision Curve Analysis (DCA) diagrams for the nomogram predict OS at 1-year, 2-year, and 3-years.

of EIF2Ss expression may be involved with tumor progression. Patients with PD also presented with high EIF2S1 and EIF2S2 levels, suggesting that overexpression of EIF2Ss may enhance tumor progression. Together, these findings implicate the EIF2Ss gene family in the malignant evolution of PAAD, and suggest that EIF2Ss expression has prognostic and diagnostic utility in this disease.

The present study, also revealed for the first time a close relationship between EIF2Ss family members and immune infiltration. Our findings indicate that high EIF2S1, EIF2S2 and EIF2S3 expression are associated with the infiltration of Th2 cells. The participation of Th2 cells in humoral immunity is closely correlated with poor prognosis in PAAD [33,34]. Th2 cells have been shown to prompt

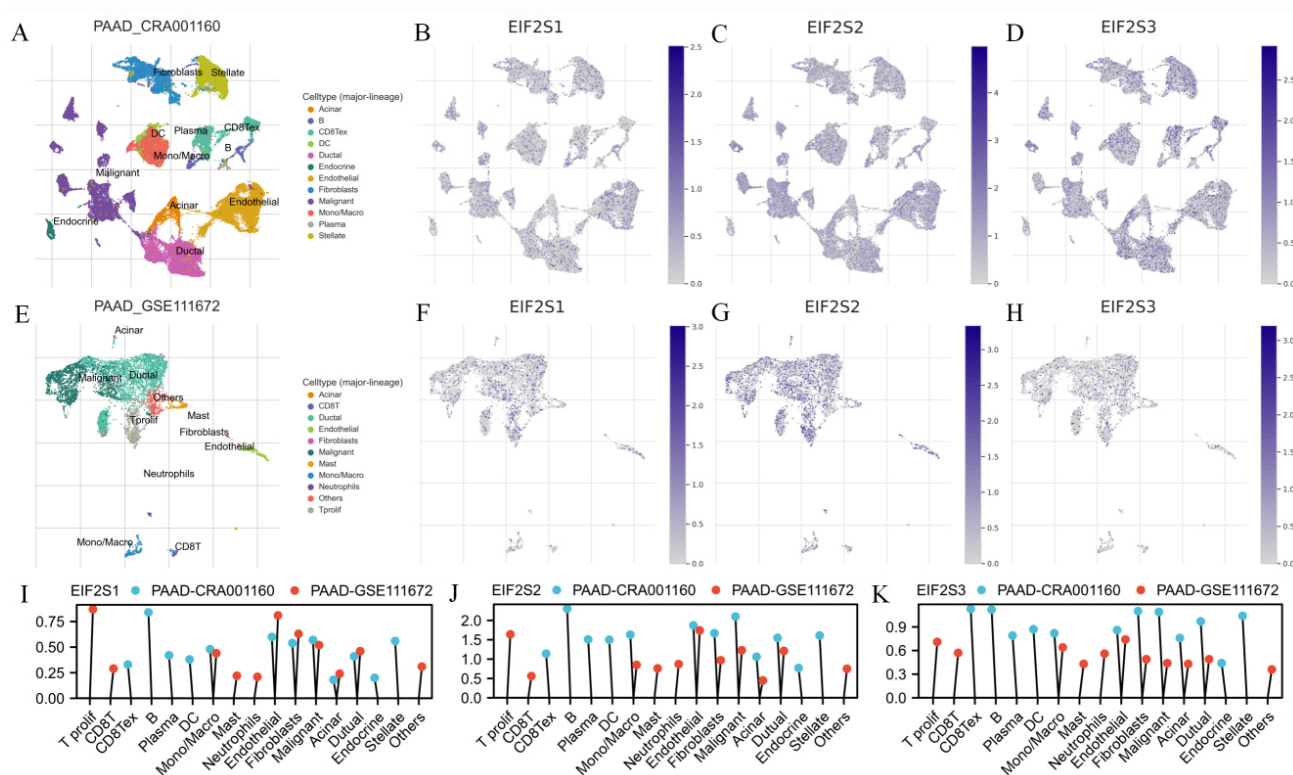


Fig. 6. ScRNA-Seq analysis of EIF2S1, EIF2S2, and EIF2S3 in PAAD. (A) The t-SNE projection of all cells in scRNA-Seq data of PAAD_CRA001160. (B–D) The expression of EIF2S1, EIF2S2, and EIF2S3 in scRNA-Seq data of PAAD_CRA001160. (E) The t-SNE projection of all cells in scRNA-Seq data of PAAD_GSE111672. (F–H) The expression of EIF2S1, EIF2S2, and EIF2S3 in scRNA-Seq data of PAAD_GSE111672. (I–K) Cells enrichment for EIF2S1, EIF2S2, and EIF2S3 in scRNA-Seq data of PAAD_CRA001160 and PAAD_GSE111672.

the tumorigenesis of pancreatic cancer via enhanced DC capacity [35]. Collectively, these results suggest that elevated expression of EIF2Ss in PAAD may contribute to the infiltration and migration of Th2 cells. In contrast, low expression of EIF2Ss in PAAD was associated with infiltration of pDC cells. In human metastatic melanoma, increased pDC cell infiltration is associated with improved survival and anti-tumor immunity [36,37]. Compared to conventional dendritic cells, pDCs were closely correlated with better DSS and DFS, tumor-infiltrating lymphocytes, and cancer immunity in PAAD [38]. Moreover, it has also been reported that pDCs enhance anti-cancer immunity when combined with anti-PD-L1 antibodies in triple negative breast cancer [39]. Together, these findings indicate that low expression of EIF2Ss and infiltration with pDC cells may improve the efficacy of immunotherapy and increase OS in some tumors types. TIMER database analysis revealed the EIF2Ss expression level was positively correlated with CD8+ T cell infiltration. CD8+ T cells are effector toxic T cells and participate in the killing of tumor cells [40–42]. CD8+ T cells have also been reported to favor an antitumor response by altering the TME and increasing the efficacy of immunotherapy [43–45]. Furthermore, changing the TME in PAAD can significantly improve therapeutic

efficacy and therefore also the prognosis of the disease. [46]. Thus, further research is warranted regarding possible correlations between EIF2Ss expression, TME and response to immunotherapy.

The present study is also the first to correlate the expression of EIF2Ss with 70 common immune checkpoints. Our results indicate that NT5E, ULBP1, PVR, CD44, IL10RB, and CD276 are all positively correlated with the expression of EIF2S1, EIF2S2, and EIF2S3. Of note, a close association was observed between EIF2Ss and the CD276 and CD44 immune checkpoints, both of which are cancer stem cell markers involved in the early growth and metastasis of tumors [47,48]. CD276 and CD44 are also closely associated with escape from immunosurveillance by cancer stem cells [49,50]. Immune checkpoint inhibitors, such as PD-I, PD-L1, CTLA-4 and others are only weakly associated with the clinical response to treatments for PAAD [51,52]. Other immune checkpoint inhibitors that target cancer stem cells, such as CD276 and CD44, may be more relevant for the treatment of PAAD.

EIF2Ss were further analyzed in the present study by using scRNA-Seq data. The PAAD_CRA001160 and PAAD_GSE111672 datasets revealed that EIF2S1, EIF2S2, EIF2S3 were all highly expressed in endothelial cells, fi-

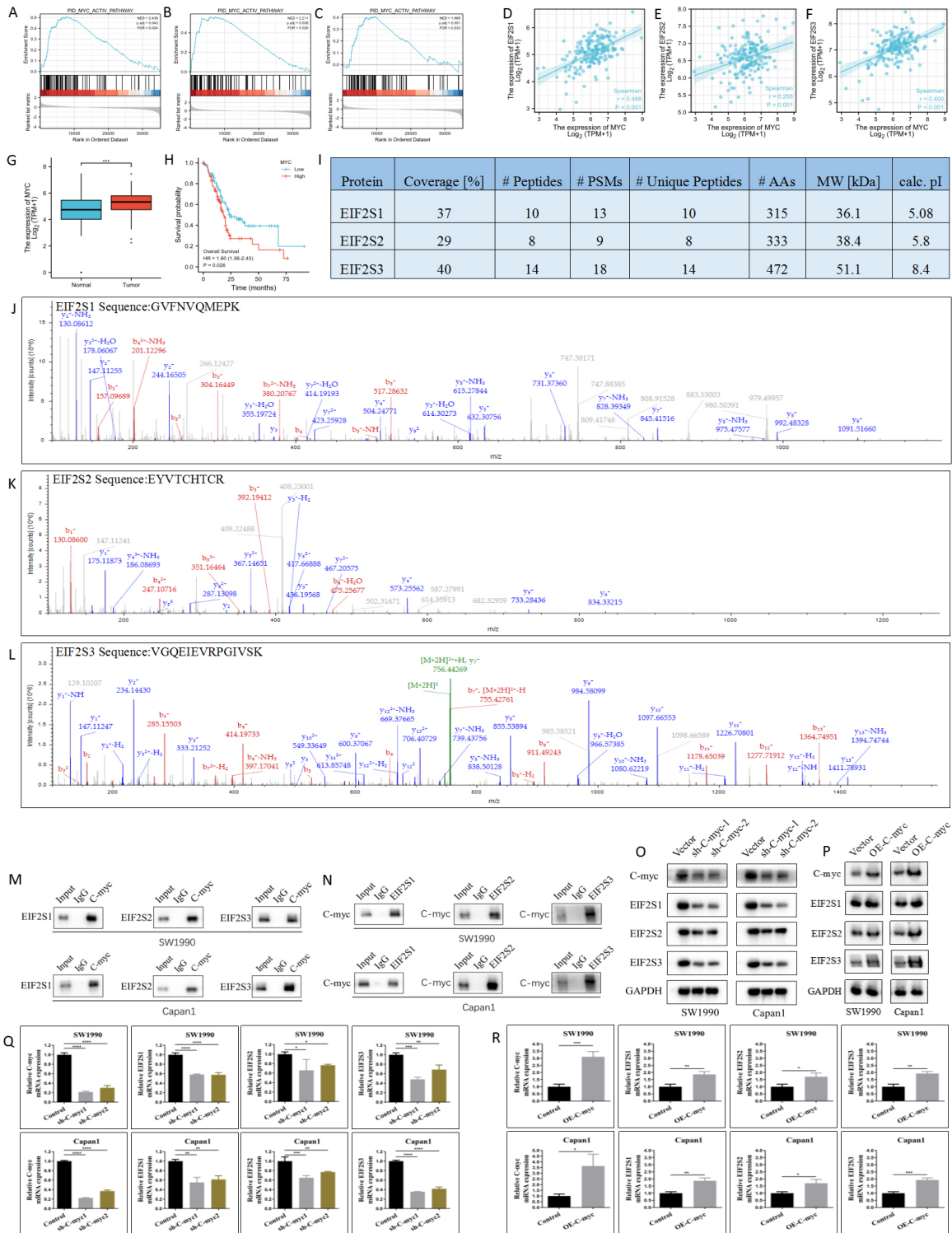


Fig. 7. Correlation of EIF2Ss with c-myc in PAAD. (A–C) GSEA functional enrichment analysis of EIF2Ss. (D–F) Spearman value correlation coefficients for EIF2S1, EIF2S2, and EIF2S3 with c-myc. (G) Upregulated of myc in pancreatic cancer tissue compared with normal tissue. (H) Kaplan–Meier survival analysis for myc expression in PAAD patients. (I) The mass spectrum assay confirmed co-immunoprecipitation of myc with EIF2S1, EIF2S2, and EIF2S3. (J–L) The mass spectrogram of EIF2S1, EIF2S2, and EIF2S3. (M,N) Co-immunoprecipitation of myc with EIF2Ss. (O) Knockdown of c-myc decreased the expression of EIF2S1, EIF2S2, and EIF2S3 (western blot results). (P) Overexpression of c-myc increased the expression of EIF2S1, EIF2S2, and EIF2S3 (western blot results). (Q) Knockdown of c-myc decreased the expression of c-myc, EIF2S1, EIF2S2, and EIF2S3 (RT-qPCR results). (R) Overexpression of c-myc increased the expression of c-myc, EIF2S1, EIF2S2, and EIF2S3 (RT-qPCR results).

broblasts, malignant cells and ductal cells. A poor immune microenvironment was found to be closely related to malignant cells, cancer-associated fibroblasts (CAF), and some tumor-infiltrating lymphocytes (TILs) [53–55]. These cells may promote tumor progression, metastasis, and poor response to immunotherapy in PAAD [56,57]. Thus, altering the immune microenvironment could benefit PAAD patients that have high EIF2Ss expression. In the current study, scRNA-seq analysis also revealed that the malignant cells with high EIF2Ss expression were mainly enriched with targets for *myc*. The functional enrichment of EIF2Ss was shown to be closely related to the *myc* pathway. Further research on the interaction between EIF2Ss and *c-myc* is therefore warranted. Mass spectrometry and western blotting confirmed that EIF2Ss co-immunoprecipitated with *c-myc*. Moreover, western blot results showed the expression of EIF2Ss was regulated by *c-myc*. Knockdown of *c-myc* in PAAD cells downregulated the expression of EIF2Ss, whereas overexpression of *c-myc* upregulated the expression of EIF2Ss. Meanwhile, these findings were also confirmed at the transcriptional level by RT-qPCR. These results suggest that PAAD patients with high EIF2Ss expression may benefit from targeted *c-myc* treatment. Therefore, it is important to detect the level of EIF2Ss expression in pancreatic cancer tissues, as this may have implications for its treatment. However, whether there are also correlations between EIF2Ss and *c-myc* in other cell types in the TME requires further investigation. In summary, targeted therapy against EIF2Ss may be beneficial for PAAD patients.

The present study has some limitations. First, the mechanism responsible for the overexpression of EIF2Ss in PAAD requires further research. Second, the accuracy and utility of the predictive model in clinical practice needs further verification. Finally, more research is needed to determine the efficacy of immunotherapy in PAAD patients with high expression of EIF2Ss.

5. Conclusions

In this study, EIF2Ss were found to be overexpressed in PAAD patients and to be associated with poor prognosis. EIF2Ss expression in PAAD was positively correlated with TILs, chemokines, and immune checkpoints. Moreover, a prognosis model consisting of EIF2Ss and important clinical characteristics showed excellent predictive value for OS in PAAD. Importantly, this research is the first to show that knockdown of *c-myc* expression can downregulate the expression of EIF2Ss in PAAD. Overall, these results demonstrate the involvement of EIF2Ss in the diagnosis, prognosis, and treatment of PAAD, and should prompt further clinical studies involving this gene family.

Availability of Data and Materials

The data used to support the findings of this study are available from corresponding author upon request.

Author Contributions

ZCao and ZChen designed and organized this study. ZCao drafted the manuscript and analyzed the data. YJ analyzed the data and supervised the study. CC conceived and revised the manuscript. FW, MG, and LR made an acquisition of the data and collected literature. ZChen, KZ, and JJ analyzed and edited the manuscript. All authors read and approved the final manuscript. All authors have participated sufficiently in the work and agreed to be accountable for all aspects of the work.

Ethics Approval and Consent to Participate

Not applicable.

Acknowledgment

The authors thank all database and analysis tools used in this study.

Funding

This work was supported by the National Natural Science Foundation of China (No. 81930115).

Conflict of Interest

The authors declare no conflict of interest.

Supplementary Material

Supplementary material associated with this article can be found, in the online version, at <https://doi.org/10.31083/j.fbl2903119>.

References

- [1] Casolino R, Corbo V, Beer P, Hwang CI, Paiella S, Silvestri V, *et al.* Germline Aberrations in Pancreatic Cancer: Implications for Clinical Care. *Cancers*. 2022; 14: 3239.
- [2] Rahib L, Smith BD, Aizenberg R, Rosenzweig AB, Fleshman JM, Matrisian LM. Projecting cancer incidence and deaths to 2030: the unexpected burden of thyroid, liver, and pancreas cancers in the United States. *Cancer Research*. 2014; 74: 2913–2921.
- [3] Zou S, Wang X, Chen H, Lin J, Wen C, Zhan Q, *et al.* Post-operative hyperprogression disease of pancreatic ductal adenocarcinoma after curative resection: a retrospective cohort study. *BMC Cancer*. 2022; 22: 649.
- [4] Tsujimae M, Masuda A, Ikegawa T, Tanaka T, Inoue J, Toyama H, *et al.* Comprehensive Analysis of Molecular Biologic Characteristics of Pancreatic Ductal Adenocarcinoma Concomitant with Intraductal Papillary Mucinous Neoplasm. *Annals of Surgical Oncology*. 2022; 29: 4924–4934.
- [5] Kanda T, Wakiya T, Ishido K, Kimura N, Fujita H, Yoshizawa T, *et al.* Heterogeneity of metabolic adaptive capacity affects the prognosis among pancreatic ductal adenocarcinomas. *Journal of Gastroenterology*. 2022; 57: 798–811.
- [6] Laurella LC, Mirakian NT, Garcia MN, Grasso DH, Sülsen VP, Papademetrio DL. Sesquiterpene Lactones as Promising Candidates for Cancer Therapy: Focus on Pancreatic Cancer. *Molecules*. 2022; 27: 3492.
- [7] Koltai T, Reshkin SJ, Carvalho TMA, Di Molfetta D, Greco MR, Alfaraouk KO, *et al.* Resistance to Gemcitabine in Pancre-

atic Ductal Adenocarcinoma: A Physiopathologic and Pharmacologic Review. *Cancers*. 2022; 14: 2486.

- [8] Chang H, Jiang S, Ma X, Peng X, Zhang J, Wang Z, *et al.* Proteomic analysis reveals the distinct energy and protein metabolism characteristics involved in myofiber type conversion and resistance of atrophy in the extensor digitorum longus muscle of hibernating Daurian ground squirrels. *Comparative Biochemistry and Physiology. Part D, Genomics & Proteomics*. 2018; 26: 20–31.
- [9] Mikami S, Masutani M, Sonenberg N, Yokoyama S, Imataka H. An efficient mammalian cell-free translation system supplemented with translation factors. *Protein Expression and Purification*. 2006; 46: 348–357.
- [10] Langland JO, Jacobs BL. Inhibition of PKR by vaccinia virus: role of the N- and C-terminal domains of E3L. *Virology*. 2004; 324: 419–429.
- [11] You K, Wang L, Chou CH, Liu K, Nakata T, Jaiswal A, *et al.* QRICH1 dictates the outcome of ER stress through transcriptional control of proteostasis. *Science*. 2021; 371: eabb6896.
- [12] Dey S, Tameire F, Koumenis C. PERK-ing up autophagy during MYC-induced tumorigenesis. *Autophagy*. 2013; 9: 612–614.
- [13] Zhang L, Zhou H, Li J, Wang X, Zhang X, Shi T, *et al.* Comprehensive Characterization of Circular RNAs in Neuroblastoma Cell Lines. *Technology in Cancer Research & Treatment*. 2020; 19: 1533033820957622.
- [14] Borek G, Shin BS, Stiller B, Mimouni-Bloch A, Thiele H, Kim JR, *et al.* eIF2 γ mutation that disrupts eIF2 complex integrity links intellectual disability to impaired translation initiation. *Molecular Cell*. 2012; 48: 641–646.
- [15] Li H, Chen S, Mi H. A Multiomics Profiling Based on Online Database Revealed Prognostic Biomarkers of BLCA. *BioMed Research International*. 2022; 2022: 2449449.
- [16] Zhang J, Li S, Zhang L, Xu J, Song M, Shao T, *et al.* RBP EIF2S2 Promotes Tumorigenesis and Progression by Regulating MYC-Mediated Inhibition via FHIT-Related Enhancers. *Molecular Therapy*. 2021; 29: 886.
- [17] Kotzaeridou U, Young-Baird SK, Suckow V, Thornburg AG, Wagner M, Harting I, *et al.* Novel pathogenic EIF2S3 missense variants causing clinically variable MEHMO syndrome with impaired eIF2 γ translational function, and literature review. *Clinical Genetics*. 2020; 98: 507–514.
- [18] Moortgat S, Manfroid I, Pendeville H, Freeman S, Bourdouxhe J, Benoit V, *et al.* Broadening the phenotypic spectrum and physiological insights related to EIF2S3 variants. *Human Mutation*. 2021; 42: 827–834.
- [19] Rohozinski J, Edwards CL. Does *EIF2S3* Retrogene Activation Regulate Cancer/Testis Antigen Expression in Human Cancers? *Frontiers in Oncology*. 2020; 10: 590408.
- [20] Söylemez Z, Arikan ES, Solak M, Arikan Y, Tokyol Ç, Şeker H. Investigation of the expression levels of CPEB4, APC, TRIP13, EIF2S3, EIF4A1, IFN γ , PIK3CA and CTNNA1 genes in different stage colorectal tumors. *Turkish Journal of Medical Sciences*. 2021; 51: 661–674.
- [21] Osei-Bordom DC, Serifis N, Brown ZJ, Hewitt DB, Lawal G, Sachdeva G, *et al.* Pancreatic ductal adenocarcinoma: Emerging therapeutic strategies. *Surgical Oncology*. 2022; 43: 101803.
- [22] Yau CC, Leeds J. Managing inoperable pancreatic cancer: the role of the pancreaticobiliary physician. *Frontline Gastroenterology*. 2022; 13: e88–e93.
- [23] Chantrill LA, Nagrial AM, Watson C, Johns AL, Martyn-Smith M, Simpson S, *et al.* Precision Medicine for Advanced Pancreas Cancer: The Individualized Molecular Pancreatic Cancer Therapy (IMPaCT) Trial. *Clinical Cancer Research*. 2015; 21: 2029–2037.
- [24] Götze J, Nitschke C, Uzunoglu FG, Pantel K, Sinn M, Wikman H. Tumor-Stroma Interaction in PDAC as a New Approach for Liquid Biopsy and its Potential Clinical Implications. *Frontiers in Cell and Developmental Biology*. 2022; 10: 918795.
- [25] Gregory LC, Ferreira CB, Young-Baird SK, Williams HJ, Harakalova M, van Haaften G, *et al.* Impaired EIF2S3 function associated with a novel phenotype of X-linked hypopituitarism with glucose dysregulation. *EBioMedicine*. 2019; 42: 470–480.
- [26] Hodgson G, Andreeva A, Bertolotti A. Substrate recognition determinants of human eIF2 α phosphatases. *Open Biology*. 2021; 11: 210205.
- [27] Roy S, Esmailniakooshkghazi A, Patnaik S, Wang Y, George SP, Ahrorov A, *et al.* Villin-1 and Gelsolin Regulate Changes in Actin Dynamics That Affect Cell Survival Signaling Pathways and Intestinal Inflammation. *Gastroenterology*. 2018; 154: 1405–1420.e2.
- [28] Schatz C, Sprung S, Scharfetter V, Codina-Martínez H, Lechner M, Hermsen M, *et al.* Dysregulation of Translation Factors EIF2S1, EIF5A and EIF6 in Intestinal-Type Adenocarcinoma (ITAC). *Cancers*. 2021; 13: 5649.
- [29] Pang K, Dong Y, Hao L, Shi ZD, Zhang ZG, Chen B, *et al.* ERH Interacts With EIF2 α and Regulates the EIF2 α /ATF4/CHOP Pathway in Bladder Cancer Cells. *Frontiers in Oncology*. 2022; 12: 871687.
- [30] Ji P, Wang H, Cheng Y, Liang S. Prognostic prediction and gene regulation network of *EIF2S2* in hepatocellular carcinoma based on data mining. *Journal of Gastrointestinal Oncology*. 2021; 12: 3061–3078.
- [31] Yang JW, Yuan LL, Gao Y, Liu XS, Wang YJ, Zhou LM, *et al.* ¹⁸F-FDG PET/CT metabolic parameters correlate with EIF2S2 expression status in colorectal cancer. *Journal of Cancer*. 2021; 12: 5838–5847.
- [32] Chang YT, Huang CS, Yao CT, Su SL, Terng HJ, Chou HL, *et al.* Gene expression profile of peripheral blood in colorectal cancer. *World Journal of Gastroenterology*. 2014; 20: 14463–14471.
- [33] Alam A, Levanduski E, Denz P, Villavicencio HS, Bhatta M, Alhorebi L, *et al.* Fungal mycobiome drives IL-33 secretion and type 2 immunity in pancreatic cancer. *Cancer Cell*. 2022; 40: 153–167.e11.
- [34] De Monte L, Wörmann S, Brunetto E, Heltai S, Magliacane G, Reni M, *et al.* Basophil Recruitment into Tumor-Draining Lymph Nodes Correlates with Th2 Inflammation and Reduced Survival in Pancreatic Cancer Patients. *Cancer Research*. 2016; 76: 1792–1803.
- [35] Zhu Y, Zhang C, Zhao D, Li W, Zhao Z, Yao S, *et al.* BDNF Acts as a Prognostic Factor Associated with Tumor-Infiltrating Th2 Cells in Pancreatic Adenocarcinoma. *Disease Markers*. 2021; 2021: 7842035.
- [36] Monti M, Vescovi R, Consoli F, Farina D, Moratto D, Berruti A, *et al.* Plasmacytoid Dendritic Cell Impairment in Metastatic Melanoma by Lactic Acidosis. *Cancers*. 2020; 12: 2085.
- [37] Zhang W, Lim SM, Hwang J, Ramalingam S, Kim M, Jin JO. Monophosphoryl lipid A-induced activation of plasmacytoid dendritic cells enhances the anti-cancer effects of anti-PD-L1 antibodies. *Cancer Immunology, Immunotherapy: CII*. 2021; 70: 689–700.
- [38] Plesca I, Benešová I, Beer C, Sommer U, Müller L, Wehner R, *et al.* Clinical Significance of Tumor-Infiltrating Conventional and Plasmacytoid Dendritic Cells in Pancreatic Ductal Adenocarcinoma. *Cancers*. 2022; 14: 1216.
- [39] Oshi M, Newman S, Tokumaru Y, Yan L, Matsuyama R, Kalinski P, *et al.* Plasmacytoid Dendritic Cell (pDC) Infiltration Correlate with Tumor Infiltrating Lymphocytes, Cancer Immunity, and Better Survival in Triple Negative Breast Cancer (TNBC) More Strongly than Conventional Dendritic Cell (cDC). *Cancers*. 2020; 12: 3342.
- [40] Elia I, Rowe JH, Johnson S, Joshi S, Notarangelo G, Kurmi K, *et al.* Tumor cells dictate anti-tumor immune responses by altering

- pyruvate utilization and succinate signaling in CD8⁺ T cells. *Cell Metabolism*. 2022; 34: 1137–1150.e6.
- [41] Guan L, Wu B, Li T, Beer LA, Sharma G, Li M, *et al.* HRS phosphorylation drives immunosuppressive exosome secretion and restricts CD8⁺ T-cell infiltration into tumors. *Nature Communications*. 2022; 13: 4078.
- [42] Zöphel D, Angenendt A, Kaschek L, Ravichandran K, Hof C, Janku S, *et al.* Faster cytotoxicity with age: Increased perforin and granzyme levels in cytotoxic CD8⁺ T cells boost cancer cell elimination. *Aging Cell*. 2022; 21: e13668.
- [43] Jin X, Hu Z, Sui Q, Zhao M, Liang J, Liao Z, *et al.* A Novel Prognostic Signature Revealed the Interaction of Immune Cells in Tumor Microenvironment Based on Single-Cell RNA Sequencing for Lung Adenocarcinoma. *Journal of Immunology Research*. 2022; 2022: 6555810.
- [44] Lefler JE, MarElia-Bennett CB, Thies KA, Hildreth BE, 3rd, Sharma SM, Pitarresi JR, *et al.* STAT3 in tumor fibroblasts promotes an immunosuppressive microenvironment in pancreatic cancer. *Life Science Alliance*. 2022; 5: e202201460.
- [45] Ye J, Mills BN, Qin SS, Garrett-Larsen J, Murphy JD, Uccello TP, *et al.* Toll-like receptor 7/8 agonist R848 alters the immune tumor microenvironment and enhances SBRT-induced antitumor efficacy in murine models of pancreatic cancer. *Journal for Immunotherapy of Cancer*. 2022; 10: e004784.
- [46] Brouwer TP, de Vries NL, Abdelaal T, Krog RT, Li Z, Ruano D, *et al.* Local and systemic immune profiles of human pancreatic ductal adenocarcinoma revealed by single-cell mass cytometry. *Journal for Immunotherapy of Cancer*. 2022; 10: e004638.
- [47] Pustovalova M, Blokhina T, Alhaddad L, Chigasova A, Chuprov-Netochin R, Veviorskiy A, *et al.* CD44⁺ and CD133⁺ Non-Small Cell Lung Cancer Cells Exhibit DNA Damage Response Pathways and Dormant Polyploid Giant Cancer Cell Enrichment Relating to Their p53 Status. *International Journal of Molecular Sciences*. 2022; 23: 4922.
- [48] Wang C, Li Y, Jia L, Kim JK, Li J, Deng P, *et al.* CD276 expression enables squamous cell carcinoma stem cells to evade immune surveillance. *Cell Stem Cell*. 2021; 28: 1597–1613.e7.
- [49] Kesharwani P, Chadar R, Sheikh A, Rizg WY, Safhi AY. CD44-Targeted Nanocarrier for Cancer Therapy. *Frontiers in Pharmacology*. 2022; 12: 800481.
- [50] Shi J, Zhao H, Lian H, Ke L, Zhao L, Wang C, *et al.* CD276 (B7H3) improve cancer stem cells formation in cervical carcinoma cell lines. *Translational Cancer Research*. 2021; 10: 65–72.
- [51] Lenzo FL, Kato S, Pabla S, DePietro P, Nesline MK, Conroy JM, *et al.* Immune profiling and immunotherapeutic targets in pancreatic cancer. *Annals of Translational Medicine*. 2021; 9: 119.
- [52] Xiang Z, Li J, Zhang Z, Cen C, Chen W, Jiang B, *et al.* Comprehensive Evaluation of Anti-PD-1, Anti-PD-L1, Anti-CTLA-4 and Their Combined Immunotherapy in Clinical Trials: A Systematic Review and Meta-analysis. *Frontiers in Pharmacology*. 2022; 13: 883655.
- [53] Chijimatsu R, Kobayashi S, Takeda Y, Kitakaze M, Tatekawa S, Arai Y, *et al.* Establishment of a reference single-cell RNA sequencing dataset for human pancreatic adenocarcinoma. *iScience*. 2022; 25: 104659.
- [54] Huang H, Wang Z, Zhang Y, Pradhan RN, Ganguly D, Chandra R, *et al.* Mesothelial cell-derived antigen-presenting cancer-associated fibroblasts induce expansion of regulatory T cells in pancreatic cancer. *Cancer Cell*. 2022; 40: 656–673.e7.
- [55] Schalck A, Sakellariou-Thompson D, Forget MA, Sei E, Hughes TG, Reuben A, *et al.* Single-Cell Sequencing Reveals Trajectory of Tumor-Infiltrating Lymphocyte States in Pancreatic Cancer. *Cancer Discovery*. 2022; 12: 2330–2349.
- [56] De Monte L, Reni M, Tassi E, Clavenna D, Papa I, Recalde H, *et al.* Intratumor T helper type 2 cell infiltrate correlates with cancer-associated fibroblast thymic stromal lymphopoietin production and reduced survival in pancreatic cancer. *The Journal of Experimental Medicine*. 2011; 208: 469–478.
- [57] Han S, Fu D, Tushoski GW, Meng L, Herremans KM, Riner AN, *et al.* Single-cell profiling of microenvironment components by spatial localization in pancreatic ductal adenocarcinoma. *Theranostics*. 2022; 12: 4980–4992.